

Feature article

Stimuli-responsive conjugated rod-coil block copolymers: Synthesis, morphology, and applications

Wen-Chung Wu^a, Ching-Yi Chen^b, Wen-Ya Lee^c, Wen-Chang Chen^{c,*}^a Department of Chemical Engineering, National Cheng Kung University, Tainan 701, Taiwan^b Department of Chemical Engineering, National Chung Cheng University, Chiayi 621, Taiwan^c Department of Chemical Engineering, National Taiwan University, Taipei 106, Taiwan

ARTICLE INFO

Article history:

Received 25 November 2014

Received in revised form

8 March 2015

Accepted 12 March 2015

Available online 20 March 2015

Keywords:

Stimuli-responsive

Conjugated rod-coil

Block copolymer

ABSTRACT

Stimuli-responsive conjugated rod-coil block copolymers have received extensive attention recently because the stimuli-responsive coils, which undergo structure, shape, and property changes as triggered by external signals. They also take the advantages of conjugated rods, which provide tunable structural control and photophysical properties due to their π – π interaction. This review focuses on the recent progress in stimuli-responsive conjugated rod-coil block copolymers on their synthetic routes, stimuli-induced transitions in morphologies, and numerous applications in different fields. We first provide an overview on synthetic methods to prepare copolymers with two major architectures: linear and hyperbranched copolymers. Moreover, the effects of different stimuli on their morphological transitions and their corresponding photophysical properties are summarized. Finally, the promising applications of these block copolymers based on single or multiple stimuli-responsive systems are discussed and highlighted for “intelligent” sensory device and biomedical systems for theranostics.

© 2015 Elsevier Ltd. All rights reserved.

1. Introduction

Stimuli-responsive polymers exhibiting a significant and reversible property transition in response to specific stimuli have recently been employed to build smart sensory devices for electronic, environmental, and biomedical applications [1–11]. The property transition of such polymers could be triggered either by an environmental parameter (e.g., temperature, pH, or redox potential) [12–14] or by an external stimulus (e.g., light or magnetic field) [15,16]. Furthermore, the development of block copolymers (BCP) with stimuli-responsive characteristics has emerged as a new platform of smart nanomaterials due to the tunable morphologies governed by various structural parameters, including architectures, relative block fractions, block polarities, and processing conditions, etc.

The morphologies of block copolymers and their consequent physical properties have attracted both fundamental and application interests in recent decades [17–28]. Tremendous efforts have been dedicated to the investigation of BCP from the establishment of new synthetic strategies, fundamental studies of self-assembly

behaviors to the applications in nanotechnologies. Various block copolymers composed of different constructed blocks and with different architectures have been successfully prepared and explored in details [29,30]. For instance, the unique molecular structures of amphiphilic block copolymers containing hydrophilic and hydrophobic segments with distinct natures between two blocks on the same polymer chains stimulate interesting and unique phase behaviors in nanometer dimensions [31–34]. The well-defined nanostructures of amphiphilic block copolymers give rise to broad applications ranging from traditional polymer technologies (thermoplastic elastomers, surfactants, and adhesives) to modern applications (semiconductors and drug delivery systems) [35–38].

Rod-coil block copolymers with rigid segments as the rod blocks, such as peptides, liquid crystals, stiff helical structures or conjugated components, have been shown to possess distinct properties as compared to conventional coil–coil block copolymers [39–48]. Among them, conjugated rod-coil block copolymers have attracted extensive research interest because the electronic and optoelectronic properties could be tuned by the nanostructures [49–55]. These special structures suppress the unfavorable macrophase separation encountered in many polymer blends while presents unique microphase separation with the formation of highly ordered geometries or patterns at nanoscales, which may

* Corresponding author. Tel.: +886 2 23628398; fax: +886 2 23623040.

E-mail address: chenwc@ntu.edu.tw (W.-C. Chen).

lead to additional electronic processes such as exciton confinement and interfacial effects [56]. The photophysical properties can also be tuned through charge-transfer and energy-transfer interactions by selecting the proper luminescent rod segments [57]. Furthermore, rod-coil block copolymers with a wide variety of architectures have been prepared by delicate synthetic routes, including rod-block-coil, rod-block-coil-block-coil, coil-block-rod-block-coil, rod-block-coil-block-rod, rod-graft-coil, and hyperbranched copolymers. These copolymers with different architectures have been demonstrated to afford various morphologies, such as micelles, vesicles, thin films, bulk samples nanofibers, and nanowires, which consequently showed superior manipulation on optoelectronic properties through morphology control [52]. Therefore, the preparation of conjugated rod-coil block copolymers opens a new channel to manipulate the optoelectronic properties of conjugated materials and the resulted device performance.

The combination of conjugated rod segments with stimuli-responsive coil chains has emerged as a radically growing field to pursue multifunctional materials with novel applications. The aim of this article is to provide a systematic overview and propose future prospects on the development of stimuli-responsive conjugated rod-coil block copolymers. Special emphasis will be put on the current challenges including synthetic approaches for the precise control over chemical structures and polymer architectures, stimuli-induced transition in morphologies and physical properties, and potential applications in different fields.

2. Synthesis of stimuli-responsive conjugated rod-coil block copolymers

Conventional coil-coil block copolymers are usually prepared either by living ionic polymerization or controlled radical polymerization of constituting monomers. However, considering the unique chemical structures of conjugated rod-coil block copolymers, the rod and coil blocks have to be constructed by different polymerization approaches, and a specific approach is used to facilitate the connection between the rod and coil blocks. The preparation of conjugated rod blocks could be accomplished by conventional coupling reactions, such as the Suzuki-Miyaura or Yamamoto coupling for poly(*para*-phenylene) (PPP) and polyfluorene (PF) [58], the Grignard metathesis method for polythiophene (PT) [59], and the Hagihara method for poly(*para*-phenyleneethynylene) [60], etc. These coupling reactions facilitate the polymerization of aromatic monomers via the condensation between specific functional groups with particular transition-metal catalytic systems. On the other hand, coil blocks are prepared by conventional addition polymerization, such as anionic living polymerization or controlled radical polymerization. The stimuli-responsive characteristics are usually introduced to coil blocks by selecting suitable monomers with desired response triggered by specific stimulus, as summarized in Fig. 1.

Considering the approaches to connect the conjugated rod and coil blocks, there are two major categories of synthetic routes for preparing the block copolymers: (i) polymerization using macroinitiators (also known as the grafting-from methods), and (ii) coupling between the preformed rod and coil blocks (also known as the grafting-onto methods) [52]. For the grafting-from method, one of the blocks is polymerized first and end-functionalized with suitable functional groups to facilitate the growth of the other block as the initiator. In the grafting-onto method, the rod and coil blocks are prepared separately and decorated with suitable functional groups which can be coupled together via a specific reaction route. For both the grafting-from and the grafting-onto methods, precise synthesis of stimuli-responsive conjugated rod-coil block copolymers with well-defined structures relies on the fidelity of the

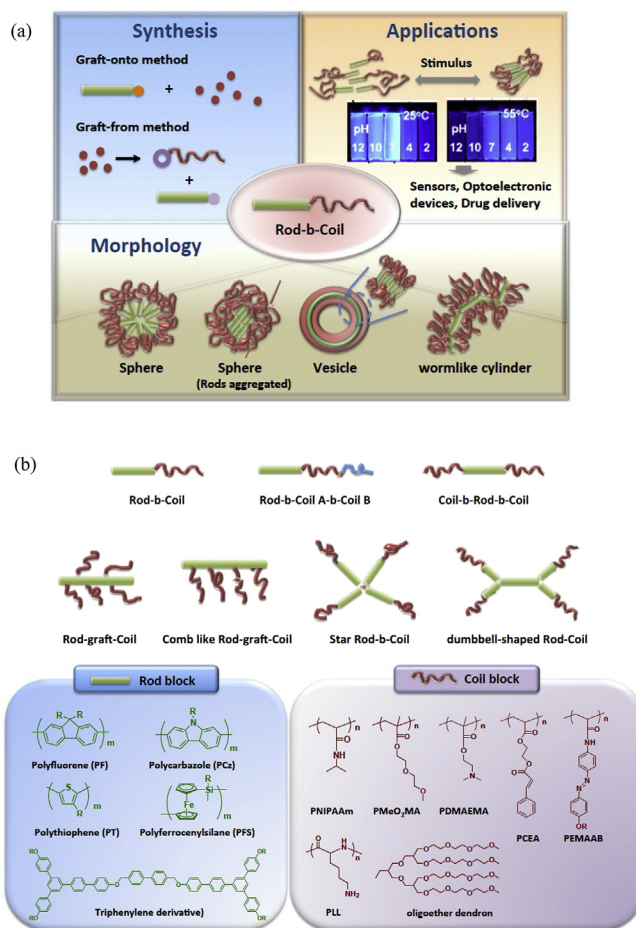


Fig. 1. A schematic diagram representing the synthetic methods, morphologies and applications of stimuli-responsive conjugated rod-coil block copolymers (a); architectures and chemical structures of stimuli-responsive conjugated rod-coil block copolymers (b). Inserted image is reproduced with the permission from Ref. [62]. Copyright 2008, the Royal Society of Chemistry.

end functionalities. For example, a significant drawback of the grafting-onto method is that the end-functional groups are in a very low concentration, which typically causes the low yield of coupling between rod and coil segments and the presence of homopolymer as impurity [55].

In the following sections, we overview the synthetic approaches according to the two major architectures of stimuli-responsive conjugated rod-coil block copolymer: (i) linear block copolymers, including rod-coil diblock copolymers and coil-rod-coil or rod-coil-coil triblock copolymers; and (ii) hyperbranched copolymers, including graft copolymers and star copolymers.

2.1. Synthesis of linear stimuli-responsive conjugated rod-coil block copolymers

2.1.1. The grafting-from method

The critical issue for the grafting-from method is the preparation of conjugated rod-like polymers with specific end functional groups, which can play the role of initiator for the sequential polymerization of the coil blocks. The controlled radical polymerization and living anionic polymerization are two typical mechanisms that have been widely used to synthesize rod-coil block copolymers. Among them, the atom transfer radical polymerization (ATRP) technique has been widely used to establish various

architectures of block copolymers due to its superior capability for polymerizing various monomer structures and also high tolerances to reaction conditions and medium polarity. The suitable end-functionalities for initiating ATRP are the aliphatic bromides, especially the tertiary bromides. Fig. 2 shows a typical synthetic scheme for preparing poly[2,7-(9,9-dihexylfluorene)]-*block*-poly(*N*-isopropylacrylamide) (PF-*b*-PNIPAAm) [61]. The rod-like PF blocks were prepared by the Suzuki coupling reaction of the fluorene monomers substituted with bromide and the boronic acid at 2 and 7 positions, respectively. The resultant rod blocks were functionalized by a two-step process to afford the desired tertiary bromides as the end groups. In the final step, the thermo-responsive PNIPAAm coil blocks were prepared by ATRP using the PF rods as macroinitiator. Similar approaches had been utilized to synthesize various stimuli-responsive conjugated rod-coil diblock copolymers with different combination of the rod and coil blocks, such as poly[2,7-(9,9-dihexylfluorene)]-*block*-poly[(2-dimethylamino)ethyl methacrylate] (PF-*b*-PDMAEMA) [62], poly(3-hexylthiophene)-*block*-poly[(2-dimethylamino)ethyl methacrylate] (P3HT-*b*-PDMAEMA) [63]. In addition to the rod-coil diblock copolymers, coil-rod-coil and rod-coil-coil triblock copolymers had also been prepared by the grafting-from routes. For example, Huang and coworkers synthesized polyfluorenes based on the Yamamoto coupling reaction and functionalized both ends with tertiary bromides [64–66]. Then, the dibromo-functionalized PF was used as the macroinitiator to prepare various stimuli-responsive coil-rod-coil triblock copolymers, including poly(methacrylic acid)-*block*-polyfluorene-*block*-poly(methacrylic acid) PMAA-*b*-PF-*b*-PMAA [64], poly[(2-dimethylamino)ethyl methacrylate]-*block*-polyfluorene-*block*-poly[(2-dimethylamino)ethyl methacrylate] (PDMAEMA-*b*-PF-*b*-PDMAEMA) [65], and poly(*N*-isopropylacrylamide)-*block*-polyfluorene-*block*-poly(*N*-isopropylacrylamide) (PNIPAAm-*b*-PF-*b*-PNIPAAm) [66]. We also prepared rod-coil-coil triblock copolymer, poly[2,7-(9,9-di-n-hexylfluorene)]-*block*-poly[poly(ethylene glycol) methyl ether methacrylate]-*block*-poly[3(triisopropoxysilyl)propyl methacrylate] (PF-*b*-PPEGMA-*b*-PPOPS), using PF macroinitiator to polymerize the two coil monomers via a one-pot ATRP route [67].

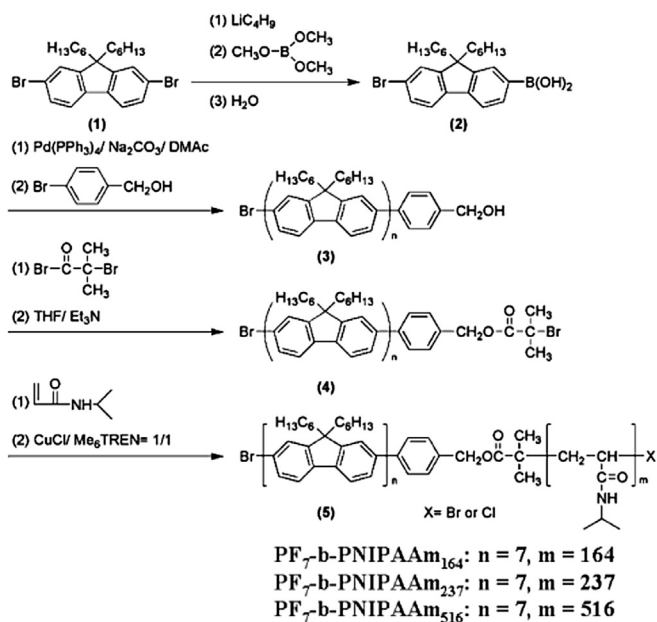


Fig. 2. Synthesis of PF-*b*-PNIPAAm rod-coil diblock copolymers via sequential Suzuki coupling reaction and ATRP [61]. Reproduced with permission. Copyright 2010, Wiley-VCH Verlag GmbH & Co.

Other polymerization routes besides ATRP have also been adapted to prepare stimuli-responsive conjugated rod-coil block copolymers with the linear architecture. Bo and his coworkers synthesized a functional coil-rod-coil triblock copolymer containing a terfluorene rod and two thermo-responsive PNIPAAm coils via reversible addition-fragmentation chain-transfer (RAFT) polymerization using terfluorene-based dithioester as the RAFT agent (Fig. 3) [68].

2.1.2. The grafting-onto method

In contrast to the grafting-from method, rod and coil segments could also be polymerized and functionalized with suitable end groups individually. Then, the corresponding conjugated rod-coil block copolymers were prepared by the condensation reactions between the respective end groups to couple the rod and coil segments. The click reaction with the advantages of simplicity, mild reaction conditions, and high conversion has been widely utilized to establish various architectures of block copolymers [69,70]. In particular, copolymers with complicated architectures, such as triblock copolymers or hyperbranched copolymers, are preferred to be prepared via the grafting-onto method, because of the difficulty of sequential polymerization using macroinitiator with a high molecular weight or sterically hindered structure. Fig. 4 represents a typical synthetic scheme for preparing rod-coil-coil triblock copolymers, polyfluorene-*block*-poly(*N*-isopropylacrylamide)-*block*-poly(*N*-methylolacrylamide) (PF-*b*-PNIPAAm-*b*-PNMA) [71]. The coil-coil diblock copolymers of PNIPAAm-*b*-PNMA with the azide end groups were prepared via a two-step ATRP to sequentially polymerize thermo-responsive PNIPAAm blocks and cross-linkable PNMA blocks using *N*-(2'-azidoethyl)-2-chloropropionamide as the initiator. Meanwhile, the rod-like polyfluorene was end-functionalized with the alkynyl group. Click reactions between the alkynyl-terminated PF and azide-terminated PNIPAAm-*b*-PNMA were performed to afford the target rod-coil-coil triblock copolymers. Similar synthetic routes were employed to synthesize linear rod-coil block copolymers with stimuli-responsive properties, such as poly[2,7-(9,9-dihexylfluorene)]-*block*-poly(*N*-isopropylacrylamide)-*block*-poly(*N*-hydroethylacrylamide) (PF-*b*-PNIPAAm-*b*-PHEAA) [72].

2.2. Synthesis of hyperbranched stimuli-responsive conjugated rod-coil block copolymers

The development of new synthetic approaches for stimuli-responsive rod-coil block copolymers with the hyperbranched architecture is of great interest from both fundamental and practical aspects [73–77]. Although the nonlinear coil-coil block copolymers have been successfully prepared and their structure-property relations were extensively investigated [78–80], the methodology for synthesizing hyperbranched conjugated rod-coil block copolymers with a well-defined architecture still remains in challenge [81,82]. Nevertheless, the morphologies and properties of hyperbranched conjugated rod-coil block copolymers are expected to be significantly different from those of their linear analogs. The interplay among polymer architectures and conformation transition of polymer chains in response to the external stimuli might open a new sight for stimuli-responsive conjugated rod-coil block copolymers. Fig. 5 demonstrates the synthetic scheme for two graft copolymers containing polythiophene as the rod block and poly(diethylene glycol methyl ethermethacrylate) and poly(oligoethylene glycol methyl ethermethacrylate) as the coil block [PT-g-PMeO₂MA (PTD) and PT-g-P(MeO₂MA-co-OEGMA) (PTDO)] based on the grafting-from method [73]. The polythiophene macroinitiator was end-functionalized with tertiary bromides at the 3 position of the

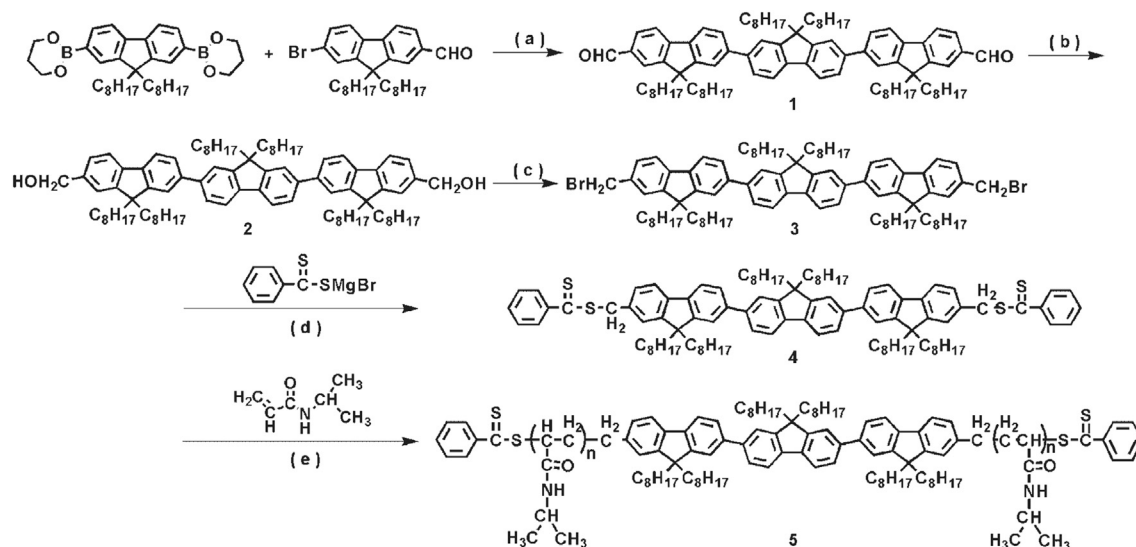


Fig. 3. Synthesis of PNIPAAm-*b*-terfluorene-*b*-PNIPAAm via RAFT [68]. Reproduced with permission. Copyright 2007, Wiley-VCH Verlag GmbH & Co.

thiophene ring, and the grafting coil blocks of P(MeO₂MA or P(MeO₂MA-co-OEGMA) were polymerized via a sequential ATRP using the polythiophene macroinitiator. Star copolymers with hyperbranched conjugated polymers as the core and thermo-responsive poly[2-(dimethylamino)ethyl methacrylate] as the arms were prepared also by the grafting-from method (HCP-*star*-PDMAEMA, Fig. 6) [74]. Similarly, the hyperbranched conjugated polymers with aldehyde terminal groups were functionalized with tertiary bromides and then utilized as the macroinitiator for the sequential ATRP to grow out the PDMAEMA arms from the core.

The synthesis of hyperbranched rod-coil block copolymers has also been accomplished by the grafting-onto method. Vancso and his coworkers reported the synthesis and characteristics of the dual responsive poly(ferrocenylsilanes) (PFS) with PNIPAAm side chains via click reaction (Fig. 7) [75]. The redox-responsive PFS backbones with pendent functional groups were prepared by the ring-opening polymerization of (3-chloropropyl)methylsilane, and a further derivation to afford pendant azide groups were

accomplished by reaction with sodium azide. The thermo-responsive PNIPAAm side chains were synthesized using *S*-1-dodecyl-*S'*-(α,α' -dimethyl- α'' -propargyl -acetate) and 3-(trimethylsilyl)prop-2-yn-1-yl-2-chloropropanoate as the alkyne-functional RAFT reagent or ATRP initiator, respectively. Lee and his coworkers prepared dumbbell-shaped amphiphiles containing poly(*p*-phenylene)-like segments as the core connected by hydrophilic and thermo-responsive oligoether coils at one end and hydrophobic dendritic alkyl coils at the other end as the asymmetric dendritic exteriors [76,77]. The synthetic route for these dumbbell-shaped amphiphiles is shown in Fig. 8 [76]. The dendritic oligoether coils (R₁) and second-generation dendritic alkyl coils (R₂) with different alkyl chain lengths were synthesized separately by the stepwise convergent approach [83], and then these two branched coils (R₁ and R₂) were incorporated onto the Y-shaped rigid aromatic segments (5 and 8a–d). The target dumbbell-shaped amphiphiles were finally obtained using 4,4'-bis(bromomethyl)-biphenyl as a bridging moiety to connect these two Y-shaped rigid aromatic segments.

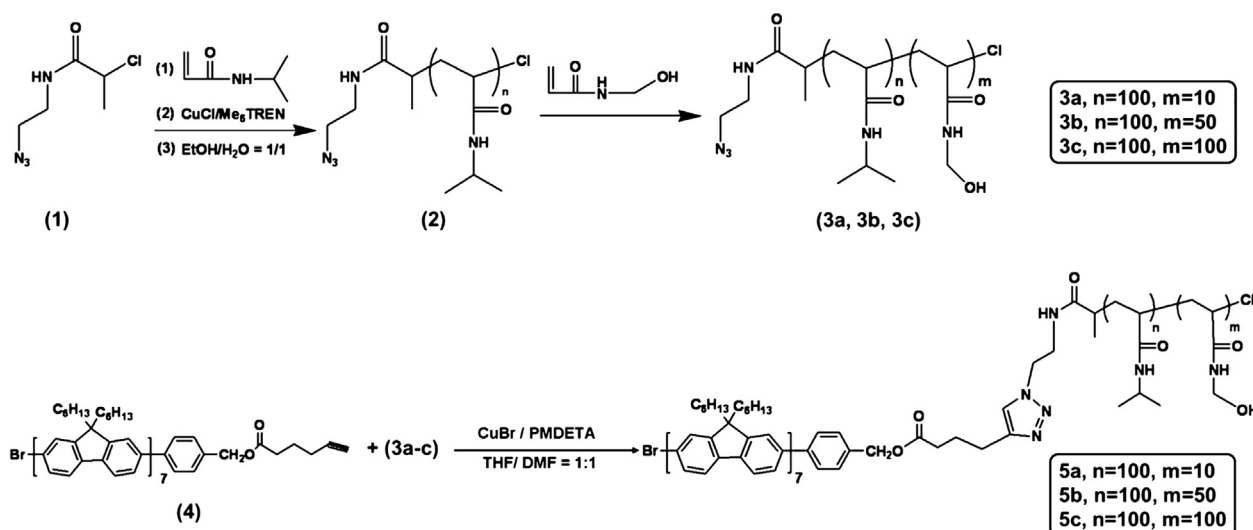


Fig. 4. Synthesis of PF-*b*-PNIPAAm-*b*-PNMA rod-coil-coil triblock copolymers. Reproduced with permission from Ref. [71]. Copyright 2012, the American Chemical Society.

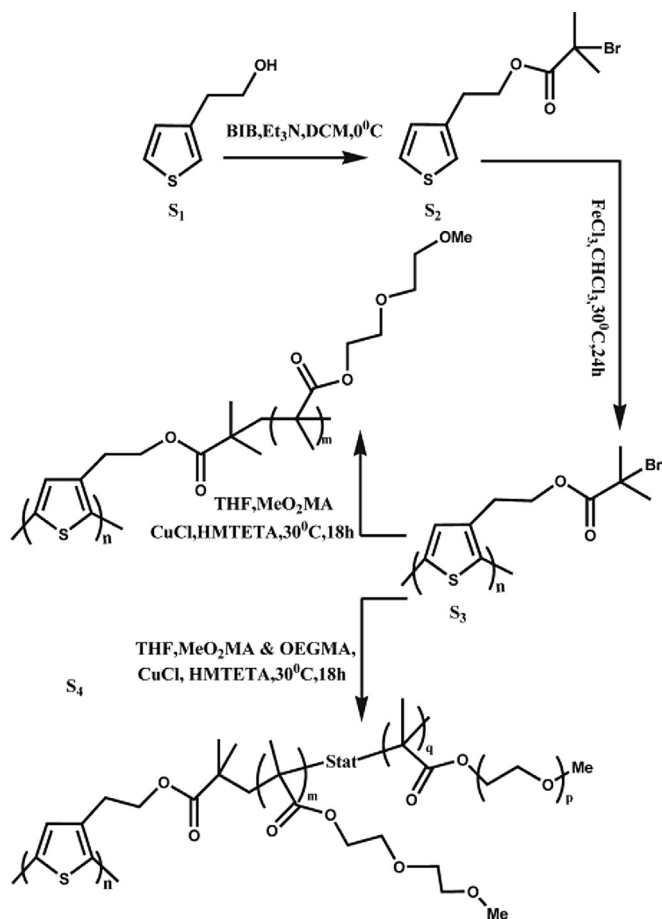


Fig. 5. Synthetic procedure adopted for the preparation of different PTD and PTDO graft copolymers. Reproduced with permission [73]. Copyright 2013, Wiley-VCH Verlag GmbH & Co.

3. Stimuli-induced transitions in morphology and their effects on photophysical properties

Stimuli-responsive materials exhibit intriguing nanostructure transitions in response to various parameters, such as temperature, pH, and light irradiation. The manipulation of block copolymer morphologies with desired conformation, size, and even functionalities is a critical challenge in consideration of finding suitable applications. The morphological control of conventional coil–coil block copolymers with stimuli-responsive characteristics and the effects of chemical structures and morphology on the photophysical properties of conjugated rod-coil block copolymers have been reviewed in several recent articles [17–22,24,26,27,32,33,39–46,52]. The replacement of one coil block with the conjugated rigid rod segment introduces new and interesting structural factors for governing the nanostructures of conjugated rod-coil block copolymers. In addition, the delicate transition of morphologies would consequently change their electronic, optical and optoelectronic properties. In this section, we focus on the effects of external stimuli on the morphological transition of stimuli-responsive conjugated rod-coil block copolymers and briefly summarize their influences on the photophysical properties.

3.1. Temperature-responsive

Thermo-responsive polymers, such as poly(*N*-isopropylacrylamide) (PNIPAAm) and poly(oligoethylene glycol

acrylate) (POEGA), form intermolecular hydrogen bonds with water molecules and possess high hydrophilicity at a low temperature, but form intramolecular hydrogen bonds among polymer chains at a high temperature. The hydrophilic–hydrophobic transition at certain critical temperatures (lower or upper critical solution temperature, LCST or UCST) would induce significant influences on the self-assembled morphologies of corresponding rod-coil copolymers. Recently, we reported several series of thermoresponsive rod-coil block copolymers with different architectures and chemical structures, including PF-*b*-PDMEMA, PF-*b*-PNIPAAm-*b*-PHEAA, P3HT-*b*-PDMAEMA, and PF-*b*-PNIPAAm-*b*-PNMA [62,63,71,72]. The LCSTs of these block copolymers showed a close correlation to their respective hydrophobic/hydrophilic block ratios. The resultant nanostructures in aqueous solutions demonstrated a wide variety of morphologies ranging from the conventional micelles to aggregated micelles, wormlike micelles and even cylindrical micelles (PF₇-*b*-PNIPAAm₁₂₀-*b*-PHEAA₃₀ in Fig. 9 as an example [72]). These morphologies showed thermoresponsive transitions based on the LCST characteristics and consequently influenced their corresponding photophysical properties, such as on/off switch of fluorescence intensity and wavelength shifts of emission peaks.

In addition to solution micelles, nanofibers based on thermoresponsive rod-coil block copolymers were successfully prepared by the electrospinning technique [61,71]. The electrospun nanofibers showed excellent wettability and dimension stability in aqueous solution via either physically blending with hydrophobic polymer or chemically crosslinked. The resultant nanofibers exhibited thermoresponsive transition in their fibrous structures which consequently changed the emissive properties. Fig. 10 shows the SEM images of the cross-linked PF₇-*b*-PNIPAAm₁₀₀-*b*-PNMA₅₀ nanofibers immersed in aqueous solutions with different temperatures [71]. The fibers swelled with water at 20 °C due to the hydrophilic PNIPAAm blocks. On the contrary, the fibers were shrunk at temperature higher than the LCST of PNIPAAm resulting from the hydrophilic–hydrophobic transition. Consequently, the fluorescence was significantly quenched for the nanofibers immersed in water at a temperature higher than LCST by comparing with those nanofibers immersed in water at a lower temperature (Fig. 11). The fluorescence quenching could be correlated to the shrinkage of fibrous structures which led to severe aggregation of PF blocks in nanofibers.

3.2. pH-responsive

pH-sensitive polymers are commonly achieved by introducing “ionizable” functional groups, such as amines, phosphoric acid and carboxylic acid, onto the polymer chains. These functional groups could be protonated or deprotonated with respective pKa values depending on the chemical structures and sequentially undergo pH-dependent transitions in physical or chemical properties. Winnik et al. reported pH-responsive rod-coil molecular brushes based on polythiophene backbone with poly(*N,N*-dimethylaminoethyl methacrylate) (PDMA) chains by the grafting-from method (PT-*g*-PDMA, Fig. 12a [84]). The copolymers exhibited a reversible pH response in aqueous solution, forming a more extended conformation while pH value decreased from 8 to 2. It is resulted from the protonation and formation of cationic quaternary amine groups and increased the repulsive interactions among the PDMA side chains. The pH-induced extended conformation drives the red shift of both absorption and PL spectra and the fluorescence quenching from the PT backbone (Fig. 12b).

Recently, Mullen et al. also established a new type of amphiphilic polyelectrolyte brushes with a rigid and hydrophobic backbone of poly(2,7-carbazole) (PC) and flexible and pH-responsive side chains of poly(L-lysine) (PLL) (PC-*g*-PLL, Fig. 13a) [85]. The PLL

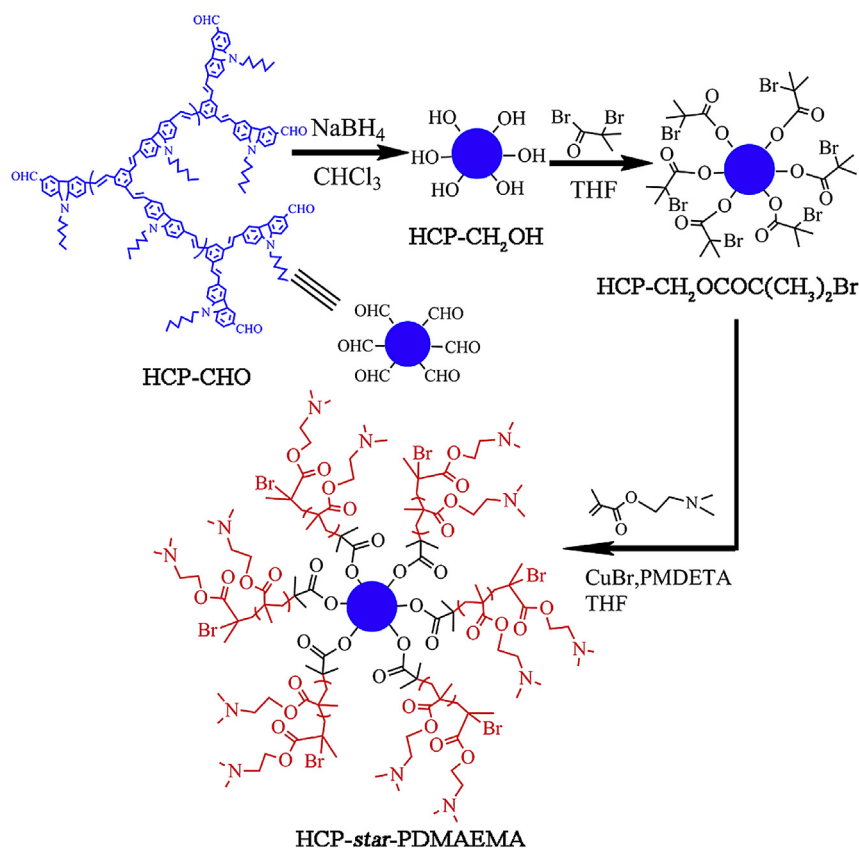


Fig. 6. Synthetic route to the HCP-star-PDMAEMA [74]. Reproduced with permission from Ref. [74]. Copyright 2013, the American Chemical Society.

side chain bearing the pendent moieties of primary amines showed the pH-induced transition between different conformations due to the protonation and deprotonation of the amino groups. As shown in Fig. 13a, the amino groups in PLL are protonated at a lower pH resulting in a rod-like conformation of PLL side chains. On the contrary, the unprotonated PLL side chains form the coil structures at higher pH values, which are the conventional structures of PLL homopolymer. From the PL spectra of PC-g-PLL at various pH values (Fig. 13b), clear pH-dependent fluorescence caused by conformational change could be observed. At a low pH condition, the fluorescence spectra show an emission peak with the maximum intensity at 425 nm and a shoulder at 460 nm. While the pH increasing, the fluorescence peak broadened significantly, and two additional maxima arose at 459 and 497 nm. The pH-dependent photoluminescence characteristics suggested that the PC backbones were aggregated in basic environments which resulted in the formation of an “excimer-like” state as indicated by the broadening of emission peak. The surface morphology of PC-g-PLL were

investigated on mica due to its negatively charged surface forming multivalent counterions for cationic PLL side chains. The AFM images exhibited untextured wormlike particles with uniform height and width but a bimodal length distribution (Fig. 13c). The formation of untextured aggregates instead of textured aggregated could be attributed to the poor solubility of hydrophobic PC backbones in aqueous solution which caused the formation of kinetically frozen aggregated on mica surface while water evaporated.

3.3. Photo-responsive

Photo-responsive polymers have been widely explored as smart materials because light irradiation is an attractive external trigger due to its spatial specificity, on/off transition, and tunable irradiation parameters (e.g. wavelength and intensity) [86,87]. The photo-responsive nanoparticles may dissolve or collapse in response to light irradiation via one of the four approaches, shifting hydrophobic-hydrophilic balance, breaking block junction, main chain degradation, and reversible cross-linking. Huang and his coworkers prepared photo-crosslinkable coil-rod-coil triblockcopolymers, poly(cinnamoyloxyethyl acrylate)-*block*-polyfluorene-*block*-poly(cinnamoyloxyethyl acrylate) (PCEA-*b*-PF-*b*-PCEA, Fig. 14a), based on the grafting method with an end-capped Yamamoto reaction and a sequential atom transfer radical polymerization [88]. These copolymers could be selectively photocrosslinked by UV irradiation via a standard photopatterning process and thus possess the potential applications in the fabrication of pixelated matrix displays and large-area displays. The crosslinking between the cinnamoyl groups could be successfully tracked by FTIR by the disappearance of the photoactive double bonds on the CEA groups. The UV-crosslinked films of these copolymers showed

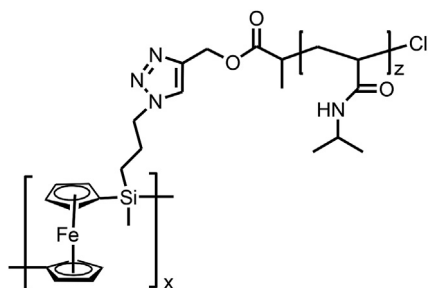


Fig. 7. Chemical structure of PFS-g-PNIPAAm prepared via the grafting onto method.

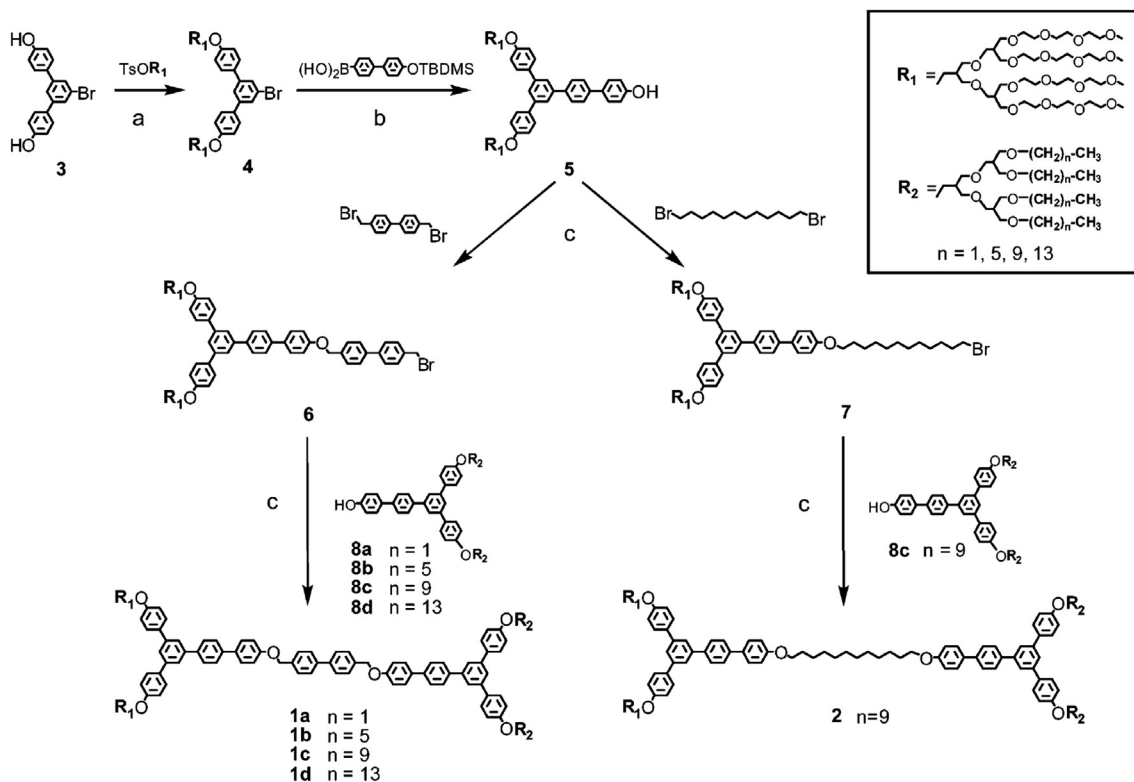


Fig. 8. Synthesis of dumbbell-shaped rod amphiphiles with thermo-responsive characteristics [76]. Reprinted with permission. Copyright 2007 American Chemical Society.

thermally stable fluorescence characteristics. By comparing the fluorescence spectra of the PF homopolymer and PCEA-*b*-PF-*b*-PCEA (Fig. 14b and c, respectively), the green emission at 530 nm was observed for PF homopolymer after annealing or UV irradiation due to aggregation, excimer formation, or fluorenone effect. On the contrary, PCEA-*b*-PF-*b*-PCEA films after thermal or UV irradiation showed only a relatively smaller peak at 530 nm. Thus, the introduction of PCEA chains could improve the stability of these fluorescent polymers.

3.4. Multi-responsive

Stimuli-responsive conjugated rod-coil block copolymers in response to more than one stimulus could be achieved by tailoring either a multi-responsive moiety or more than one type of responsive moieties onto the polymers. The delicate design of chemical structures to enable the polymers precisely responding to the target stimuli gives them potential applications in various fields. Our group reported the synthesis, nanostructures, and multifunctional sensory properties of dual-responsive rod-coil block copolymers, poly(3-hexylthiophene)-*block*-poly(2-(dimethylamino)ethyl methacrylate) (P3HT-*b*-PDMAEMA, Fig. 15a) [63]. These copolymers formed micellar structures in aqueous solutions which exhibited clear hydrophilic–hydrophobic transition in response to temperature with LCST around 33 °C (Fig. 15b). The micellar size also demonstrated a significant variation from 67 ± 8 nm to 222 ± 6 nm as the pH value is decreased from 12 to 4, due to the protonation of the PDMAEMA block at a lower pH, which led to the electrostatic repulsion between PDMAEMA chains (Fig. 15c).

Recently, Nandi et al. also explored the thermal and pH responsive characteristics of polythiophene-based graft copolymers, polythiophene-*graft*-poly[(diethyleneglycol methyl-ether methacrylate)-*co*-(*N,N*-dimethyl aminoethyl methacrylate)] [PT-*g*-P(MeO₂MA-*co*-DMAEMA) (PTDM), Fig. 16] [89]. The

nanostructures of these copolymers in aqueous solution were explored in details using DLS and TEM, and a hypothetical mechanism was proposed to explain the morphological transitions with temperature and pH. At pH of 9.2 which is higher than pKa of PDMAEMA chains and at the temperature lower than LCST of PMeO₂MA chains, PTDM copolymers self-assembled and formed micelles in aqueous solution with PT blocks aggregated in the core. The size of micelles increases dramatically as temperature was raised above the LCST of PMeO₂MA due to the collapse of PMeO₂MA chains on the insoluble PT core. On the contrary, the similar size transition was not observed in the copolymer solutions with pH of 7 or 4 which are below the pKa (~7.5) of the NMe₂ groups of PDMAEMA chains. This could be attributed to the electrostatic repulsion between protonated PDMAEMA chains at a lower pH prohibited the collapse of PMeO₂MA chains at the temperature higher than its LCST. The fluorescence intensity of the PTDM copolymer aqueous solutions at pH of 9.2 showed a significant increase with a slightly blue shift of the emission peak as temperature was increased from 22 to 29 °C, whereas the intensity and peak wavelength remained almost no change with raising temperature at pH values of 4 and 7. The transition of fluorescence characteristics for PTDMs could be well-correlated to their conformational changes in response to thermal and/or pH stimuli. At the higher pH of 9.2, the enhancement of fluorescence intensity from PT core at the temperature higher than the LCST of PMeO₂MA could be attributed to the collapse of PMeO₂MA chains on the PT core. It prevented the water molecules from getting near to the PT chains and thus reduced the possibility of nonradiative energy transfer due to solvent–solute interaction. However, the collapse of PMeO₂MA chains was prohibited by the electrostatic repulsion between protonated PDMAEMA chains at the pH value lower than its pKa. As a result, no similar variation of fluorescence intensity was observed as the micelle solution at pH 7 or 4 was heated or cooled across LCST of PMeO₂MA.

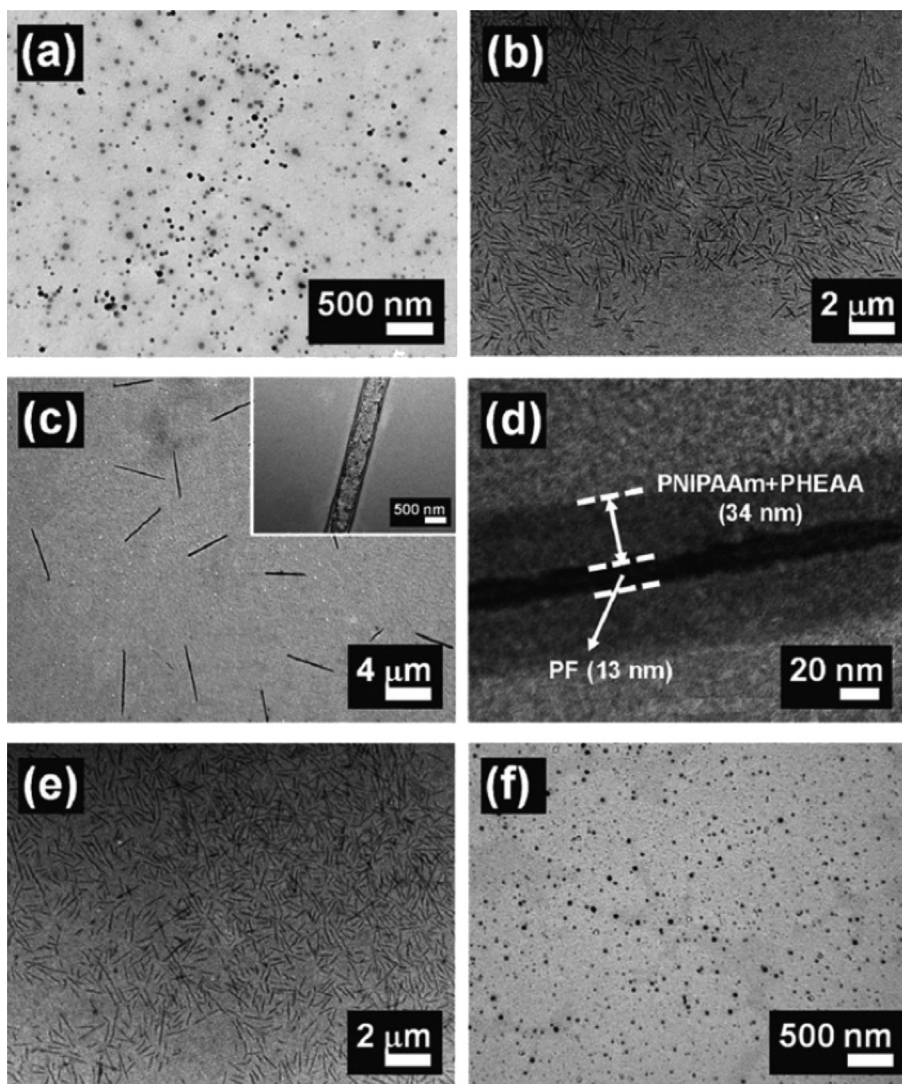


Fig. 9. Micelle morphologies of PF₇-*b*-PNIPAAm₁₂₀-*b*-PHEAA₃₀ in water during a heating-cooling cycle between 25 and 50 °C. TEM images of micelle aggregates in the heating process at (a) 25, (b) 40 and (c) 50 °C, respectively, and (d) HRTEM observation at 50 °C. TEM images of micelle aggregates in the cooling process at (e) 40 and (f) 25 °C, respectively [72]. Reproduced by permission of The Royal Society of Chemistry.

4. Applications

4.1. Sensors

For the dual-responsive conjugated rod-coil block copolymers, P3HT-*b*-PDMAEMA (Fig. 15a) [63], the conformation of copolymers

in the mixed solvent of water/THF showed transition from spherical micelles, vesicles, and finally to large spherical micelle aggregation as the solvent composition varied from 0 to 100 wt% of water. Fig. 17a represents a proposed mechanism for the conformational transition of P3HT-*b*-PDMAEMA in mixed solvent. The conformational changes induced clear changes in the photophysical

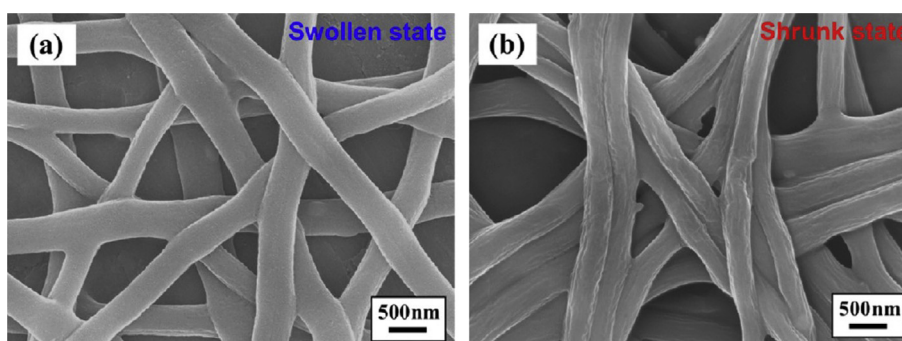


Fig. 10. FE-SEM images of the cross-linked PF₇-*b*-PNIPAAm₁₀₀-*b*-PNMA₅₀ nanofibers treated by water as temperature varied from (a) 20 to (b) 50 °C [71]. Reproduced by permission. Copyright 2012 American Chemical Society.

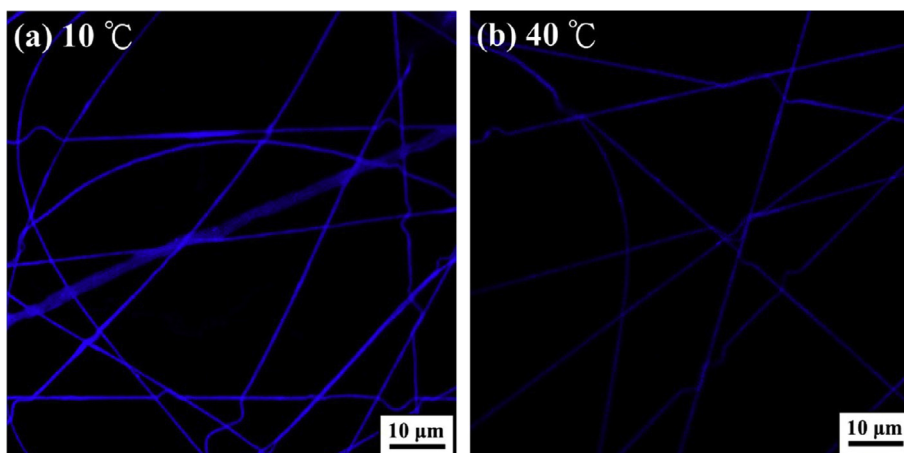


Fig. 11. Confocal images of the cross-linked PF₇-*b*-PNIPAAm₁₀₀-*b*-PNMA₅₀ nanofibers immersed in pure water at (a) 10 and (b) 40 °C [71]. Reproduced by permission. Copyright 2012 American Chemical Society.

properties [63]. Both the absorption and fluorescence spectra exhibited clear red shifts with increasing water content, and the emissive color consequently varied from yellow, orange, red to dark (Fig. 17b) [63].

The PT-based thermo and pH responsive graft copolymers, PT-*g*-P(MeO₂MA-*co*-DMAEMA) (PTDM) consist an electron rich PT core and thus possess the potential application for sensing electron deficient compounds [89]. The fluorescence spectra of the aqueous solutions of PTDM with the concentration of 0.2 vol% at pH 7.4 showed significant intensity quenching after adding various kinds

of aromatic nitro compounds (PA: picric acid, 2,4-DNP: 2,4-dinitrophenol, PNP: *p*-nitrophenol). The aromatic nitro compounds acted as electron acceptors due to their low-lying π^* orbitals and caused fluorescence quench of PTDM. The highest degree of quenching with PA is attributed to its favorable reduction potential due to a maximum number of nitro substitutions as compared to 2,4-DNP and PNP. The Stern-Volmer plot shows a linear Stern-Volmer relationship up to 63 μM of PA with a Stern–Volmer constant of $2.7 \times 10^4 \text{ M}^{-1}$. The fluorescence quench of PTDM in the solid state after contacting with PA were investigated by absorbing PTDM onto filter paper and dipped into PA solution or in contact with the PA powder. The pristine PTDM absorbed on the filter paper showed green fluorescence upon irradiation with UV light of 365 nm. After dipping the PTDM-absorbed paper into the PA solution, followed by drying, clear fluorescence was observed upon UV irradiation. Similar fluorescence quench could be demonstrated either by drop-casting a toluene solution of PA on the PTDM-absorbed paper or by direct contact with PA powder. The results suggest PTDM could be used to detect PA and possibly other nitroaromatic compounds both in the solution and in the solid state, including trinitrotoluene (TNT) or dinitrotoluene (DNT) for nitro-explosives.

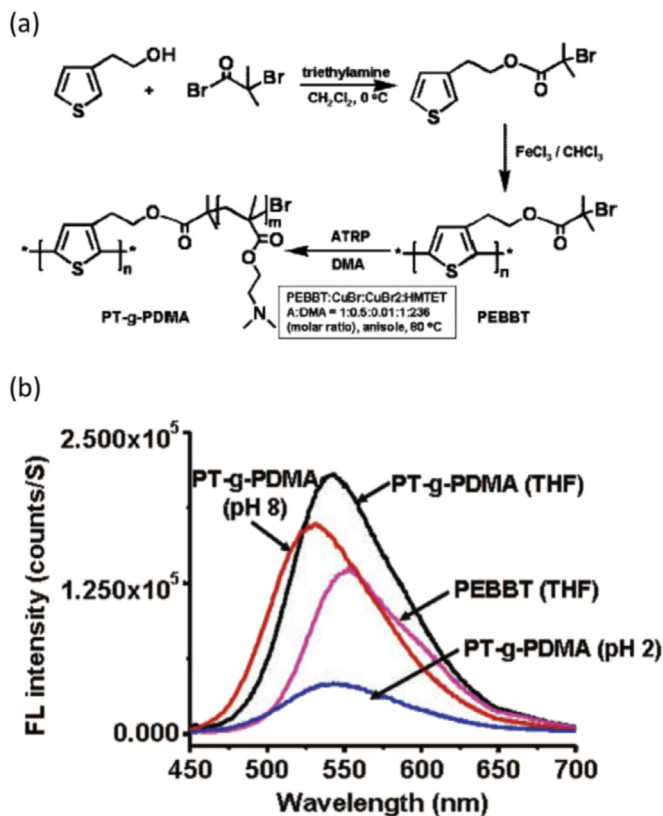


Fig. 12. Synthetic route of PT-*g*-PDMA (a); the fluorescence spectra of PEBBT macro-initiator and PT-*g*-PDMA in THF and in water with different pH values (b) [84]. Reproduced by permission. Copyright 2008 American Chemical Society.

4.2. Biomedical applications

Smart materials that exhibit nanostructural transitions in response to specific stimuli have been employed to build stimuli-responsive DDSs capable of controlled drug release [2,4,5,8,11,12,15,16,90,91]. The spatiotemporal control of drug release could be engineered to correlate with either an environmental parameter, such as temperature, pH or redox potential, or an external stimulus (e.g. light, magnetic field, or ultrasound). For instance, photo-responsive and hydrophobic moieties transit into hydrophilic upon exposure to light irradiation and thus results in the dissociation of the original self-assembled aggregates into unimers in aqueous solution. Thermo-responsive nanoparticles have also been designed based on temperature-sensitive polymers such as poly(*N*-isopropylacrylamide) (PNIPAAm) and poly(oligoethylene glycol acrylate) (POEGA), which display the hydrophilic–hydrophobic transition at their LCSTs resulting in disintegration or collapse of the thermo-responsive nanoparticles. The controlled and site-specific drug release from this type of nanoparticles can be accomplished in conjugation with hyperthermia treatment.

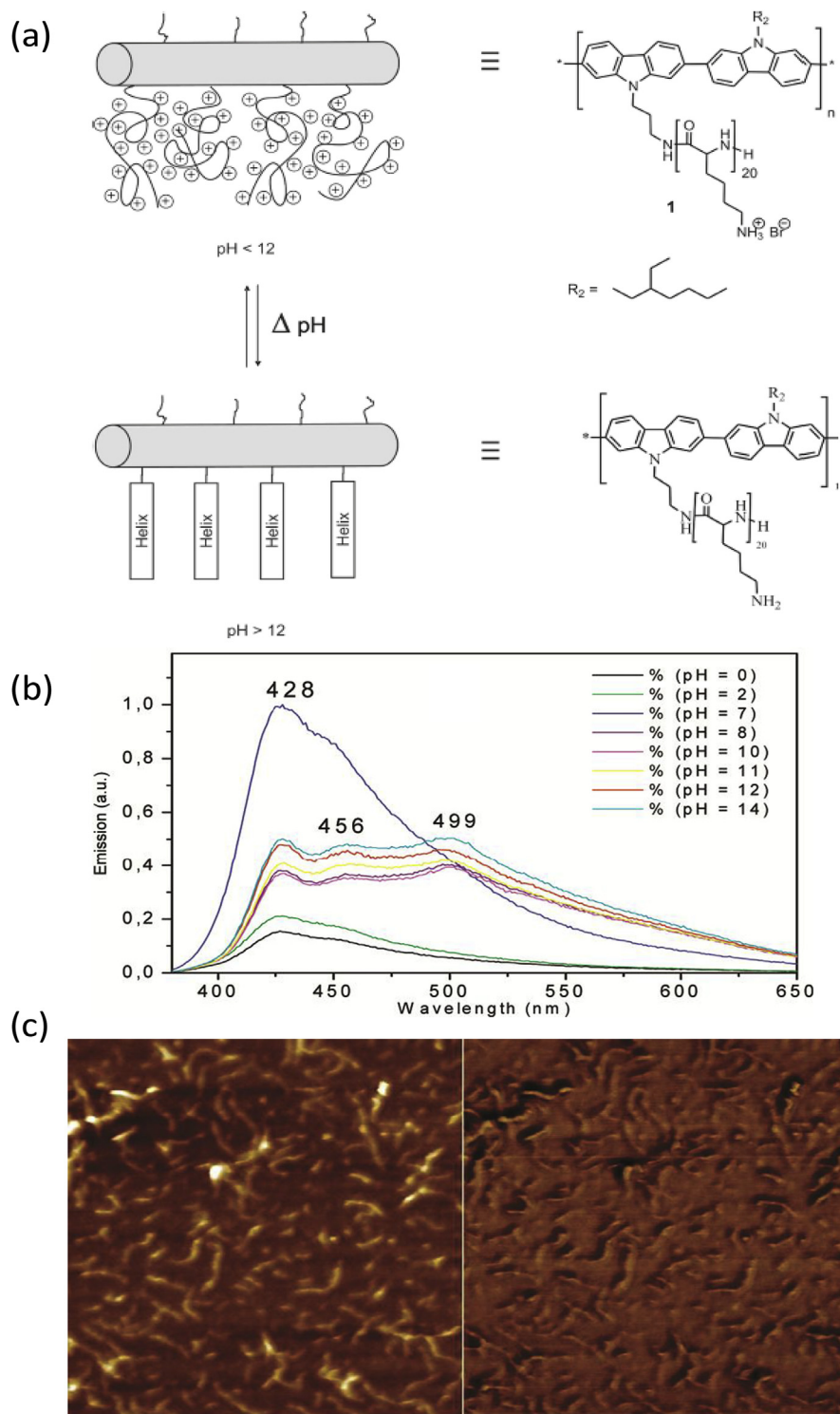


Fig. 13. Polyelectrolyte comb-like copolymers, PC-g-PLL, with a conjugated rod as the backbone and polyelectrolyte side chains (a); fluorescence spectra of PC-g-PLL aqueous solutions with different pH values (b); AFM images (left: height, right: phase) of spin-coated PC-g-PLL on mica (c) [85]. Reproduced by permission. Copyright 2013 American Chemical Society.

Jen and his coworkers prepared a series of amphiphilic rod-coil block copolymers, (PF-*b*-PNIPAAm, Fig. 18a), which self-assembled in aqueous solution and formed micellar nanostructure with PF blocks as the core and PNIPAAm blocks as the corona [92]. The micelles were used as nanocarriers to load a water-insoluble porphyrin derivative, tetrakis(mesityl)porphyrin [$\text{H}_2(\text{Me}_3)\text{TPP}$],

which is a commonly used photosensitizer in the photodynamic therapy to produce singlet oxygen by light irradiation. Fig. 18b shows the fluorescence spectra of $\text{H}_2(\text{Me}_3)\text{TPP}$ -loaded PF-*b*-PNIPAAm micelles with different loading contents. Clear fluorescence quench of PF (425 nm) with increasing loading content of $\text{H}_2(\text{Me}_3)\text{TPP}$ suggested efficient Forster resonance energy transfer

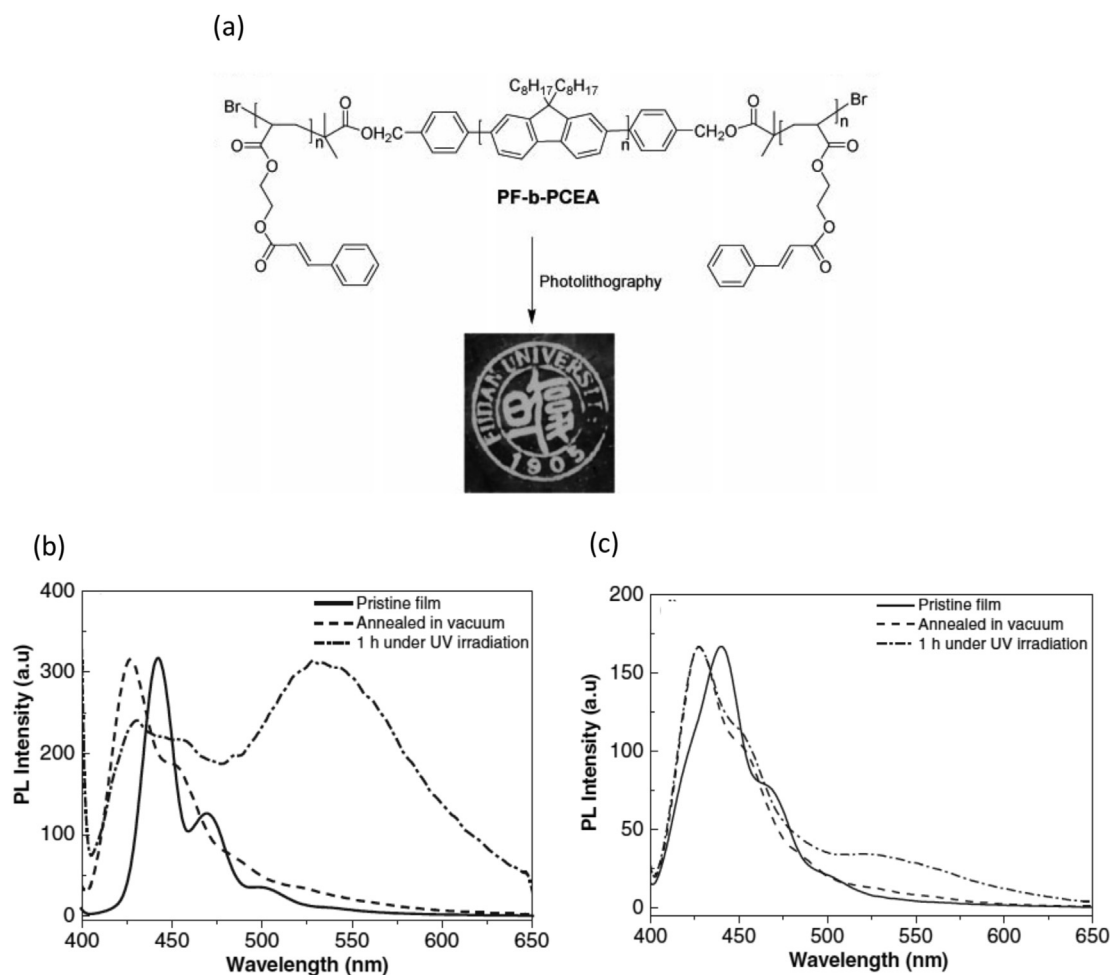


Fig. 14. Chemical structure of PF-*b*-PCEA (a); photoluminescence spectra of PFOH (b) and PF-*b*-PCEA (c) under UV irradiation for 1 h [88]. Reproduced with permission. Copyright 2006, Wiley-VCH Verlag GmbH & Co.

(FRET) from the PF cores (donor) to $H_2(Me_3)TPP$ (acceptor) due to the good spectral overlap and close proximity between PF and $H_2(Me_3)TPP$ in the cores of micelles. The rates of singlet oxygen generation were evaluated by a chemical method with the disodium salt of 9,10-anthracenedipropionic acid (ADPA). The first-order kinetic of ADPA bleaching by singlet oxygen was monitored by the absorption of ADPA, and the comparison between FRET micelles (rod-coil) and non-FRET micelles (coil-coil) was shown in Fig. 18c. The efficient FRET from PF to $H_2(Me_3)TPP$ promoted more efficient generation of singlet oxygen from $H_2(Me_3)TPP$ which was 2 times higher than those $H_2(Me_3)TPP$ molecules encapsulated in coil-coil block copolymer micelles.

Liu and his coworkers reported the preparation of highly water-soluble, neutral, fluorescent PF-based glycopolymers and demonstrated successful detection of *Escherichia coli* (*E. coli*) with this new fluorescent probe [93]. Fig. 19a shows the chemical structures of three PF-based glycopolymers with different spacers and carbohydrates substituted at the 9,9-position of fluorene moieties. Two hydrophilic oligo(ethylene glycol)- and poly(ethylene glycol)-tethered spacers were introduced to the fluorene monomers before the Suzuki coupling polymerization in order to improve water solubility for their corresponding polymers. Post functionalization of these PF-based conjugated polymers with two different carbohydrates resulted in β -glucose-bearing or α -mannose-bearing glycopolymer useful for biosensing application for bacteria. The glycopolymer with oligo(ethylene glycol)-

tethered spacers (polymer A in Fig. 19a) showed poor water solubility because the hydrophilicity of oligo(ethylene glycol) was not strong enough to suppress the π - π interaction between hydrophobic PF-based conjugated backbone. However, the glycopolymers with poly(ethylene glycol)-tethered spacers (polymer B and C in Fig. 19a) are highly water-soluble due to their long, flexible, hydrophilic spacers. The specific binding of the α -mannose-bearing glycopolymer (polymer C in Fig. 19a) with type 1 pili of *E. coli* was investigated by comparing the stain experiments with two strains of *E. coli*. One expresses the wild-type type 1 pili (ORN 178 strain) and the other expresses abnormal type 1 pili that lack the ability to mediate α -mannose-specific binding. Fig. 19b shows the fluorescent images for the *E. coli* cells of the ORN 178 strain stained with polymer C. The strong multivalent cooperative interactions between the α -mannose-bearing glycopolymer and the type 1 pili resulted in the aggregation of bacteria, forming highly fluorescent bacterial clusters as shown in the left and middle images in Fig. 19b. By contrast, the incubation of the ORN 208 strain with polymer C did not show successful stain or bacterial clusters, indicating the absence of specific binding between polymer C and the ORN 208 strain.

5. Conclusion and outlooks

Stimuli-responsive conjugated rod-coil block copolymers exhibiting switchable electronic or luminescent transitions

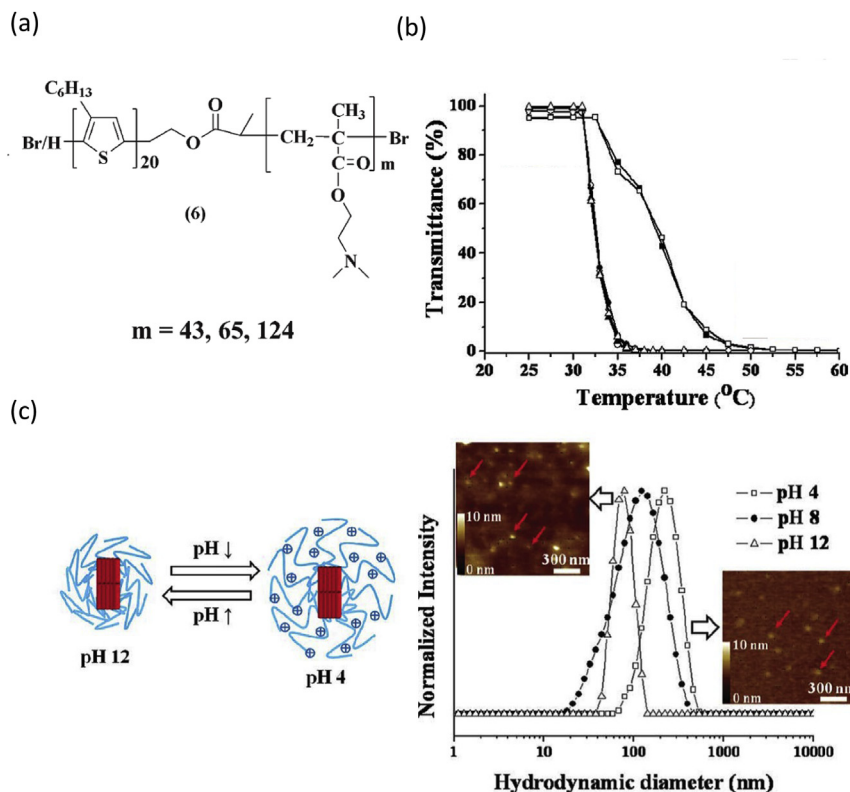


Fig. 15. Chemical structures of P3HT₂₀-*b*-PDMAEMA_m (a); Variation of transmittance with temperature for three series of P3HT-*b*-PDMAEMA (b); Size distributions and AFM images of P3HT₂₀-*b*-PDMAEMA₄₃ at different pH values with a schematic representation for pH-dependent morphologies (c) [63]. Reproduced with permission. Copyright 2011, Wiley-VCH Verlag GmbH & Co.

controlled by external stimuli open a new realm in applications, including “intelligent” sensory devices, membrane science, optoelectronic devices and biomedical applications, as summarized in Fig. 20. For further development of this new material system, design of the synthetic routes and optimization of their responsive efficiency and luminescent characteristics are crucial challenges. In addition, systematic exploration on the correlation between luminescent characteristics with the self-assembly morphologies of stimuli-responsive conjugated rod-coil block copolymers shall provide essential guidelines for both fundamental research and practical applications. From the synthetic and morphological point of view, although several linear and hyperbranched stimuli-responsive conjugated rod-coil block copolymers have been prepared based on graft-on and graft-from approaches, further efforts have to be devoted to precisely control the rod/coil compositions and molecular weight. Moreover, systematic investigation on the self-assemble morphologies, especially for the packing type of conjugated rods and exposure to the external stimuli, could be beneficial to figure out the complex photoluminescent behaviors of conjugated rod blocks in solution or solid state. Currently, exploration on the ordering of morphologies and packing type of rod blocks in solid state is still deficient, which is of great importance for their applications in optoelectronic devices.

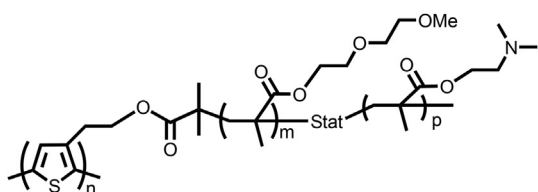


Fig. 16. Chemical structure of PT-g-P(MeO₂MA-co-DMAEMA).

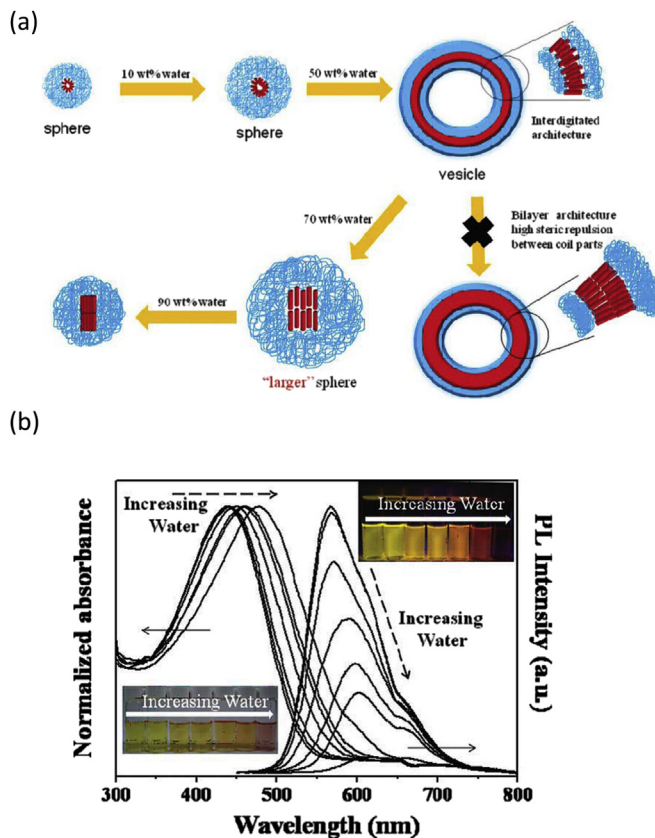


Fig. 17. A proposed mechanism for the formation of micelles and vesicles of P3HT₂₀-*b*-PDMAEMA_m (a); absorption and fluorescence spectra of P3HT₂₀-*b*-PDMAEMA₄₃ in THF/water solution with different water contents (b) [63]. Reproduced with permission. Copyright 2011, Wiley-VCH Verlag GmbH & Co.

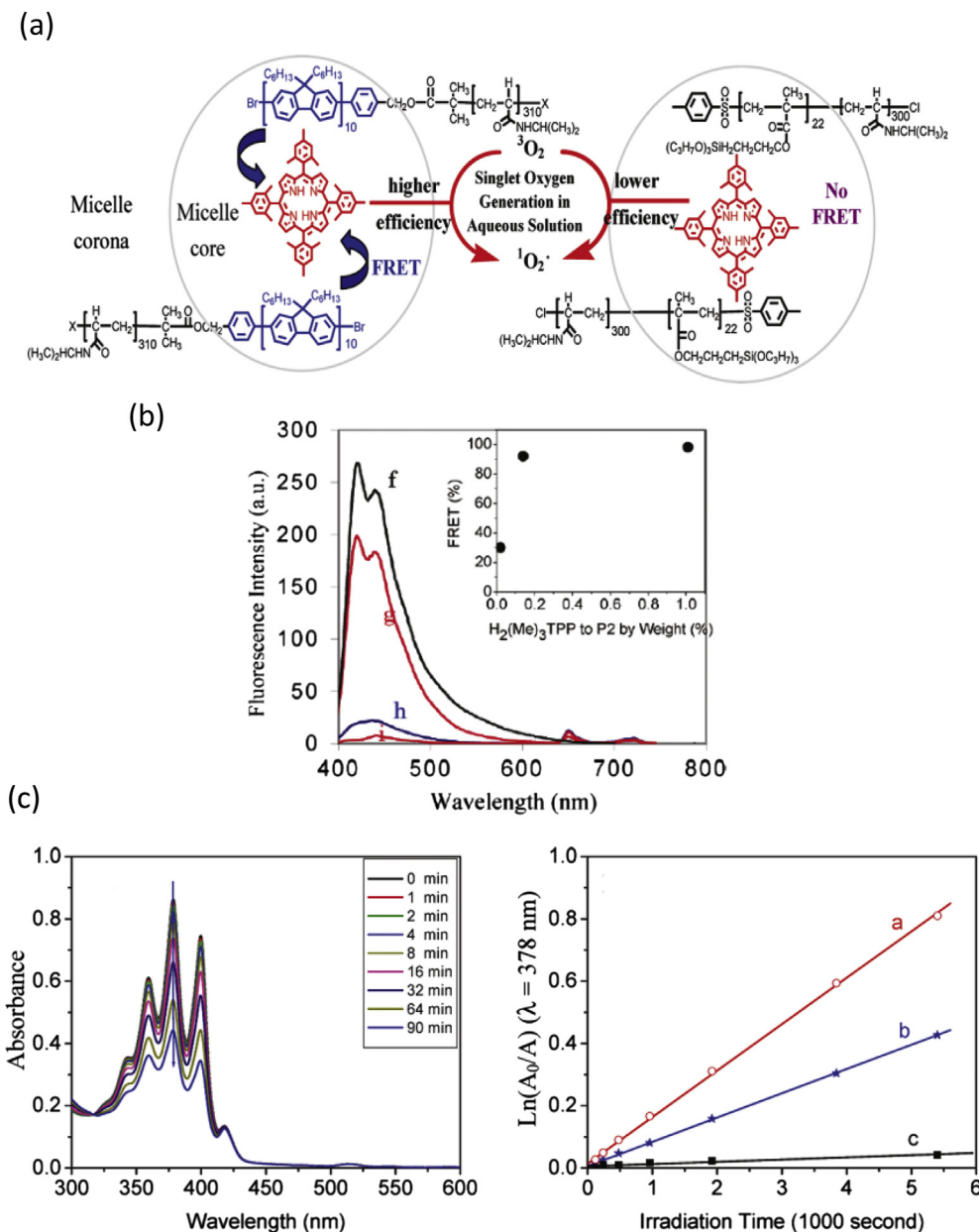


Fig. 18. A schematic representation for the use of PF-*b*-PNIPAAm to load $\text{H}_2(\text{Me}_3)\text{TPP}$ and the enhancement of singlet oxygen generation through FRET (a); fluorescence spectra of $\text{H}_2(\text{Me}_3)\text{TPP}$ -loaded PF-*b*-PNIPAAm micelles with loading ratios of 0, 0.02, 0.14, 1.01 wt% excited at 380 nm (b); investigation of singlet oxygen generation (left: typical absorption spectra at different irradiation time; right: kinetic plot with curve a of $\text{H}_2(\text{Me}_3)\text{TPP}/\text{PF-}b\text{-PNIPAAm}/\text{ADPA}$, curve b of $\text{H}_2(\text{Me}_3)\text{TPP}/\text{PPOPS-}b\text{-PNIPAAm}/\text{ADPA}$, and curve c of $\text{PF-}b\text{-PNIPAAm}/\text{ADPA}$) (c) [92]. Reproduced by permission. Copyright 2010 American Chemical Society.

For the potential applications of stimuli-responsive conjugated rod-coil block copolymers, development of “intelligent” sensory devices and membrane in solid state is receiving considerable attention. These applications take the advantages of conjugated rod blocks, especially for their mechanical superiority and amplified signal response when a small perturbation is introduced, as well as that of stimuli-responsive coils showing a reversible on/off responsiveness. The combination of the previously established conjugated polymer sensors with stimuli-responsive polymers not only provides a simple and direct strategy for developing sensory device but improve the solubility of conjugated polymers. These intelligent sensory devices would be expected to exhibit different morphologies (e.g. phase behavior, size and domain spacing) and

chain conformation (stretch/collapse) that correlated to a reversible on/off transition on photoluminescence as triggered by environmental stimuli or recognition of the analyte.

On the other hand, stimuli-responsiveness presents a pivotal property in biomedical applications due to its allowance for controllable response from biological compartments. A large variety of stimuli-responsive polymer systems has been developed for therapeutic purpose and herein introducing the luminescent rod segments expands the applications for not only diagnostic purposes but also allows for tracing the polymer systems or other specific biomolecules. However, a key issue needs to be considered prior to preparation of the block copolymers. Only biocompatible polymers can be used without toxicity problems. Finally, from

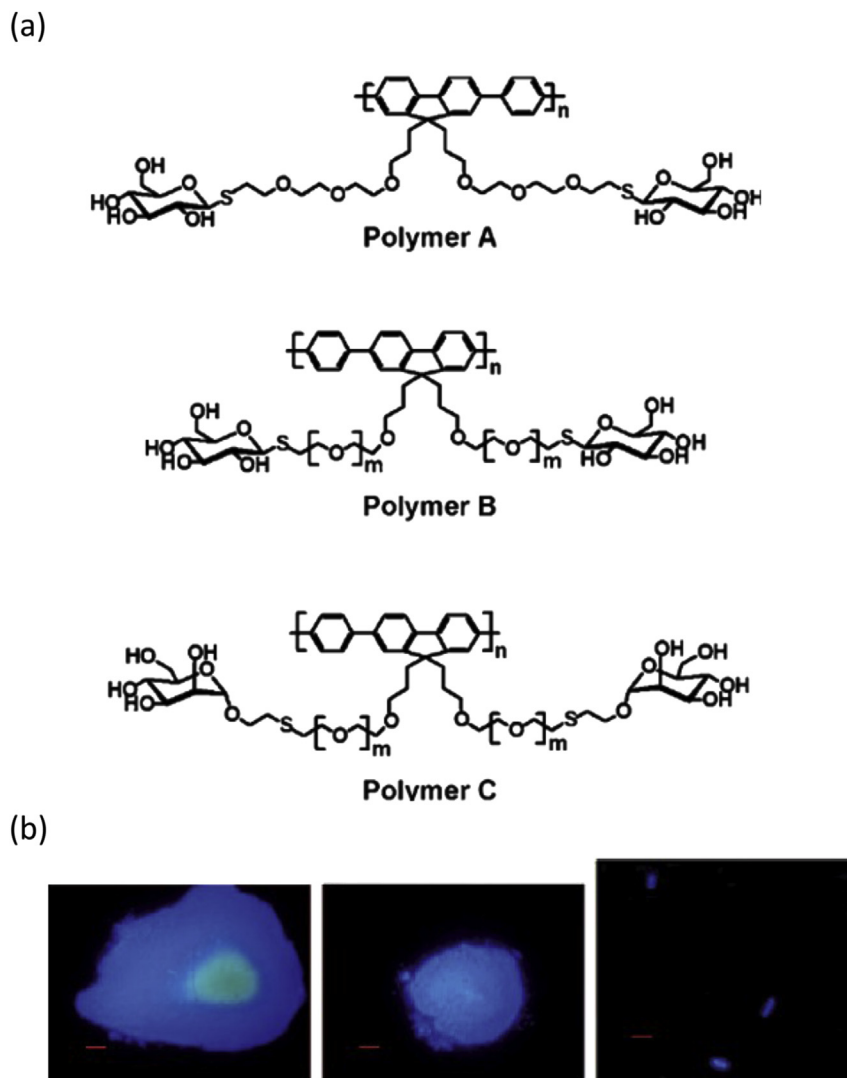


Fig. 19. Chemical structures of polyfluorene-based glycopolymers A, B and C (a); fluorescent microscopy images of fluorescent glycopolymer-stained *E. coli* bacteria cluster with 109 and 106 bacterial cells (left and middle), respectively, and fluorescent glycopolymer-stained *E. coli* bacterial cells of the ORN 178 strain (right) (b). The scale bar is 10 micron [93]. Reproduced with permission. Copyright 2009, Wiley-VCH Verlag GmbH & Co.

materials and application perspectives, many challenges remain in development of stimuli-responsive conjugated rod-coil block copolymers since it is an embryonic research field. Therefore, this review summarizes current progress on materials design,

morphological and photoluminescent tuning, and potential applications. We expect more effort would be dedicated to further development of novel stimuli-responsive conjugated rod-coil block copolymers to serve the specific devices and applications.

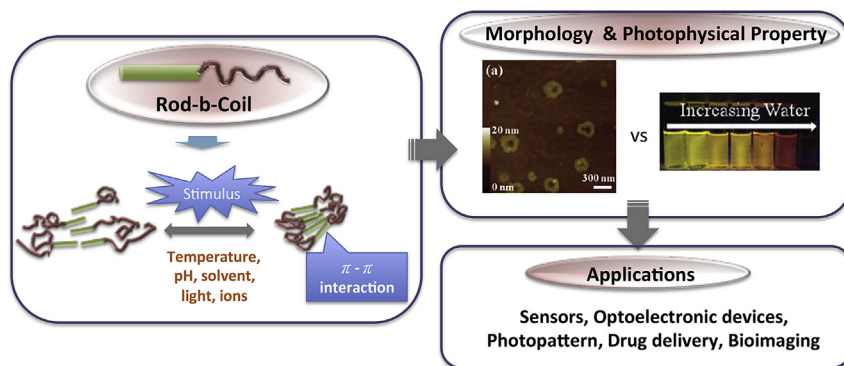


Fig. 20. Correlation between structure, morphology, photophysical properties and applications of stimuli-responsive conjugated rod-coil block copolymers. Inserted images are reproduced with permission from Ref. [63]. Copyright 2011, Wiley-VCH Verlag GmbH & Co.

Acknowledgments

The financial supports from Ministry of Science and Technology are highly appreciated.

References

- [1] Yerushalmi R, Scherz A, van der Boom ME, Kraatz H-B. *J Mater Chem* 2005;15(42):4480.
- [2] de Las Heras Alarcon C, Pennadam S, Alexander C. *Chem Soc Rev* 2005;34(3):276–85.
- [3] Dimitrov I, Trzebicka B, Müller AHE, Dworak A, Tsvetanov CB. *Prog Polym Sci* 2007;32(11):1275–343.
- [4] Ganta S, Devalapally H, Shahiwala A, Amiji M. *J Control Release* 2008;126(3):187–204.
- [5] Meng F, Zhong Z, Feijen J. *Biomacromolecules* 2009;10(2):197–209.
- [6] Li M-H, Keller P. *Soft Matt* 2009;5(5):927–37.
- [7] Kim H-J, Kim T, Lee M. *Acc Chem Res* 2011;44(1):72–82.
- [8] Calejo MT, Sande SA, Nystrom B. *Expert Opin Drug Deliv* 2013;10(12):1669–86.
- [9] Hu J, Liu S. *Acc Chem Res* 2014;47(7):2084–95.
- [10] Hu J, Zhang G, Ge Z, Liu S. *Prog Polym Sci* 2014;39(6):1096–143.
- [11] Swaminathan S, Garcia-Amoros J, Fraix A, Kandoth N, Sortino S, Raymo FM. *Chem Soc Rev* 2014;43(12):4167–78.
- [12] Chilkoti A, Dreher MR, Meyer DE, Raucher D. *Adv Drug Deliv Rev* 2002;54:613–30.
- [13] Felber AE, Dufresne MH, Leroux JC. *Adv Drug Deliv Rev* 2012;64(11):979–92.
- [14] Calejo MT, Meng F, Deng C, Feijen J, Zhong Z. *J Control Release* 2011;152(1):2–12.
- [15] Fomina N, Sankaranarayanan J, Almutairi A. *Adv Drug Deliv Rev* 2012;64(11):1005–20.
- [16] Sun C, Lee JS, Zhang M. *Adv Drug Deliv Rev* 2008;60(11):1252–65.
- [17] Moffitt M, Khougaz K, Eisenberg A. *Acc Chem Res* 1996;29(2):95–102.
- [18] Bates FS, Fredrickson GH. *Phys Today* 1999;52(2):32.
- [19] Klok H-A, Lecommandoux S. *Adv Mater* 2001;13(16):1217–29.
- [20] Fasolka MJ, Mayes AM. *Annu Rev Mater Res* 2001;31:323–55.
- [21] Forster S, Plantenberg T. *Angew Chem Int Ed* 2002;41(5):688–714.
- [22] Krausch G, Magerle R. *Adv Mater* 2002;14(21):1579–83.
- [23] Lodge TP. *Macromol Chem Phys* 2003;204(2):265–73.
- [24] Hadjichristidis N, Pispas S, Floudas CA. *Block copolymers: synthesis strategies, physical properties, and applications*. New Jersey: John Wiley & Sons Ltd; 2003.
- [25] Harrison C, Dagata JA, Adamson DH. *Developments in block copolymer science and technology*. New York: John Wiley & Sons Ltd; 2004.
- [26] Hamley I. *Block copolymers in solution: fundamentals and applications*. England: John Wiley & Sons Ltd; 2005.
- [27] Cheng JY, Ross CA, Smith HI, Thomas EL. *Adv Mater* 2006;18(19):2505–21.
- [28] He W-N, Xu J-T. *Prog Polym Sci* 2012;37(10):1350–400.
- [29] Hamley IW. *The physics of block copolymers*. New York: Oxford University Press; 1998.
- [30] Shi H, Zhao Y, Dong X, Zhou Y, Wang D. *Chem Soc Rev* 2013;42(5):2075–99.
- [31] Förster S, Antonietti M. *Adv Mater* 1998;10(3):195–217.
- [32] Alexandridis P, Lindman B. *Amphiphilic block copolymers: selfassembly and applications*. Amsterdam: Elsevier; 2001.
- [33] Zhang J, Chen XF, Wei HB, Wan XH. *Chem Soc Rev* 2013;42(23):9127–54.
- [34] Barthel MJ, Schacher FH, Schubert US. *Polym Chem* 2014;5(8):2647.
- [35] Craver C, Carraher C. *Applied polymer science: 21st century*. London: Elsevier; 2000.
- [36] Mark JE, Erman B, Eiricj FR. *The science and technology of rubber*. 3rd ed. ed. London: Elsevier Academic Press; 2011.
- [37] Park M, Harrison C, Chaikin PM, Register RA, Adamson DH. *Science* 1997;276(5317):1401–4.
- [38] Kataoka K, Harada A, Nagasaki Y. *Adv Drug Deliv Rev* 2001;47(1):113–31.
- [39] Lee M, Cho B-K, Zin W-C. *Chem Rev* 2001;101(12):3869–92.
- [40] Leclere P, Hennebicq E, Calderone A, Brocogens P, Grimsdale AC, Mullen K, et al. *Prog Polym Sci* 2003;28:55–81.
- [41] Hoeberl FJM, Jonkheijm P, Meijer EW, Schenning APHJ. *Chem Rev* 2005;105(4):1491–546.
- [42] Chen P, Yang G, Liu T, Li T, Wang M, Huang W. *Polym Int* 2006;55(5):473–90.
- [43] Liang Y, Wang H, Yuan S, Lee Y, Gan L, Yu L. *J Mater Chem* 2007;17(21):2183–94.
- [44] Olsen B, Segalman R. *Mater Sci Eng R* 2008;62(2):37–66.
- [45] Lim Y-b, Moon K-S, Lee M. *J Mater Chem* 2008;18(25):2909–18.
- [46] Dolezel S, Behringer H, Schmid F. *Polym Sci Ser C* 2013;55(1):70–3.
- [47] Zhuang Z, Cai C, Jiang T, Lin J, Yang C. *Polymer* 2014;55(2):602–10.
- [48] Changez M, Kang NG, Koh HD, Lee JS. *Langmuir* 2010;26(12):9981–5.
- [49] Jenekhe SA, Chen XL. *Science* 1998;279:1903–7.
- [50] Surin M, Marsitzky D, Grimsdale AC, Mullen K, Lazzaroni R, Leclere P. *Adv Funct Mater* 2004;14(7):708–15.
- [51] Chocho CL, Tzolakis PK, Gregoriou VG, Kallitsis JK. *Macromolecules* 2004;37(7):2502–10.
- [52] Liu C-L, Lin C-H, Kuo C-C, Lin S-T, Chen W-C. *Prog Polym Sci* 2011;36:603–37.
- [53] Topham PD, Parnell AJ, Hiorns RC. *J Polym Sci B Polym Phys* 2011;49(16):1131–56.
- [54] Li W, Kim Y, Lee M. *Nanoscale* 2013;5(17):7711–23.
- [55] Yassar A, Miozzo L, Girona R, Horowitz G. *Prog Polym Sci* 2013;38(5):791–844.
- [56] Segalman RA, McCulloch B, Kirmayer S, Urban JJ. *Macromolecules* 2009;42(23):9205–16.
- [57] Tao Y, Ma B, Segalman RA. *Macromolecules* 2008;41(19):7152–9.
- [58] Cianga I, Yagci Y. *Prog Polym Sci* 2004;29(5):387–99.
- [59] Lee JU, Cirpan A, Emrick T, Russell TP, Jo WH. *J Mater Chem* 2009;19(10):1483.
- [60] Francke V, Radel HJ, Geerts Y, Mullen K. *Macromol Rapid Commun* 1998;19:275–81.
- [61] Tzeng P, Kuo C-C, Lin S-T, Chiu Y-C, Chen W-C. *Macromol Chem Phys* 2010;211(13):1408–16.
- [62] Lin S-T, Tung Y-C, Chen W-C. *J Mater Chem* 2008;18(33):3985–92.
- [63] Huang K-K, Fang Y-K, Hsu J-C, Kuo C-C, Chang W-H, Chen W-C. *J Polym Sci A Polym Chem* 2011;49(1):147–55.
- [64] Lu S, Fan Q-L, Liu S-Y, Chua S-J, Huang W. *Macromolecules* 2002;35:9875–81.
- [65] Lu S, Fan Q-L, Chua S-J, Huang W. *Macromolecules* 2003;36:304–10.
- [66] Ma Z, Qiang L, Zheng Z, Wang Y, Zhang Z, Huang W. *J Appl Polym Sci* 2008;110(1):18–22.
- [67] Wu W-C, Tian Y, Chen C-Y, Lee C-S, Sheng Y-J, Chen W-C, et al. *Langmuir* 2007;23(5):2805–14.
- [68] Xiao X, Fu Y-q, Zhou J-j, Bo Z-s, Li L, Chan C-M. *Macromol Rapid Commun* 2007;28(9):1003–9.
- [69] Pasini D. *Molecules* 2013;18(8):9512–30.
- [70] Avti PK, Maysinger D, Kakkara A. *Molecules* 2013;18(8):9531–49.
- [71] Chiu YC, Chen Y, Kuo CC, Tung SH, Kakuchi T, Chen WC. *ACS Appl Mater Interfaces* 2012;4(7):3387–95.
- [72] Lin S-T, Fuchise K, Chen Y, Sakai R, Satoh T, Kakuchi T, et al. *Soft Matt* 2009;5(19):3761–70.
- [73] Das S, Samanta S, Chatterjee DP, Nandi AK. *J Polym Sci A Polym Chem* 2013;51(6):1417–27.
- [74] Qiu F, Wang D, Wang R, Huan X, Tong G, Zhu Q, et al. *Biomacromolecules* 2013;14(5):1678–86.
- [75] Kutnyánszky E, Hempenius MA, Vancso GJ. *Polym Chem* 2014;5(3):771–83.
- [76] Lee E, Jeong Y-H, Kim J-K, Lee M. *Macromolecules* 2007;40(23):8355–60.
- [77] Lee E, Kim JK, Lee M. *Macromol Rapid Commun* 2010;31(11):975–9.
- [78] Nandan B, Lee C-H, Chen H-L, Chen W-C. *Macromolecules* 2005;38(24):10117–26.
- [79] Chiang W-S, Lin C-H, Yeh C-L, Nandan B, Hsu P-N, Lin C-W, et al. *Macromolecules* 2009;42(6):2304–8.
- [80] Hatton FL, Chambon P, McDonald TO, Owen A, Rannard SP. *Chem Sci* 2014;5(5):1844–53.
- [81] Goseki R, Hirao A, Kakimoto M-a, Hayakawa T. *ACS Macro Lett* 2013;2(7):625–9.
- [82] Grana E, Katsigiannopoulos D, Karantzalis AE, Baikousi M, Avgeropoulos A. *Euro Polym J* 2013;49(5):1089–97.
- [83] Cho B-K, Jain A, Nieberle J, Mahajan S, Wiesner U. *Macromolecules* 2004;37(11):4227–34.
- [84] Wang M, Zou S, Guerin G, Shen L, Deng K, Jones M, et al. *Macromolecules* 2008;41:6993–7002.
- [85] Fruth A, Klapper M, Müllen K. *Macromolecules* 2010;43(1):467–72.
- [86] Zhao Y. *Macromolecules* 2012;45(9):3647–57.
- [87] Zhao H, Sterner ES, Coughlin EB, Theato P. *Macromolecules* 2012;45(4):1723–36.
- [88] Qiang L, Ma Z, Zheng Z, Yin R, Huang W. *Macromol Rapid Commun* 2006;27(20):1779–86.
- [89] Das S, Chatterjee DP, Samanta S, Nandi AK. *RSC Adv* 2013;3(38):17540.
- [90] Gil E, Hudson S. *Prog Polym Sci* 2004;29(12):1173–222.
- [91] Liu J, Huang Y, Kumar A, Tan A, Jin S, Mozhi A, et al. *Biotechnol Adv* 2014;32(4):693–710.
- [92] Tian Y, Chen C-Y, Yip H-L, Wu W-C, Chen W-C, Jen AKY. *Macromolecules* 2010;43(1):282–91.
- [93] Xue C, Velayudham S, Johnson S, Saha R, Smith A, Brewer W, et al. *Chem Eur J* 2009;15(10):2289–95.



Wen-Chung Wu received his Ph. D. degree from National Taiwan University in 2006. He joined Prof. Wen-Chang Chen's group as a postdoc researcher in National Taiwan University in 2007. In 2008, he joined Prof. Alex Jen's group to continue his postdoc research in University of Washington, Seattle, US. In 2010, he became an assistant Professor in National Cheng Kung University. His current research interests include stimuli-responsive amphiphilic copolymers, polymersome-based drug delivery systems and fluorescence sensory materials.



Ching-Yi Chen received her Ph. D. degree from University of Washington, Seattle, US in 2009. After graduation, she joined Professor Alex K.-Y. Jen's group as a postdoc researcher in University of Washington in 2009. In 2010, he joined Prof. Wen-Chang Chen's group to continue her postdoc research in National Taiwan University. In 2011, she became an assistant Professor in National Chung Cheng University. Her current research focuses on development of controlled release delivery systems using stimuli-responsive polymers and multifunctional nanocarriers.



Wen-Ya Lee received his Ph. D. degree from National Taiwan University in 2009. After graduation, he joined Prof. Wen-Chang Chen's group as a postdoc researcher in National Taiwan University in 2010. In 2012, he joined Prof. Zhenan Bao's group to continue his postdoc research in Stanford University, US. In 2015, he became an assistant



Professor in National Taipei University of Technology. His current research interests include polymer-based field-effect transistors, memory and wearable electronics.

Prof. Wen-Chang Chen received his Ph.D. degree in 1993 from Department Chemical Engineering at University of Rochester, USA. After three years as a researcher at Industrial Technology Research Institute, he joined National Taiwan University (NTU) as an associate professor and was promoted to be a full professor in 2000. He was appointed as the Director of Institute of Polymers Science and Engineering of NTU (2005–2011), and Polymer Program Coordinator of National Science Council (2009–2011). Currently, he is a distinguished professor and Associate Dean of College of Engineering, NTU. His research interests include electronic and optoelectronic polymers, precise polymer synthesis, and organic-inorganic hybrid materials.